

CERN-PPE/95-66

May 4th 1995

**A STUDY OF CASCADE AND STRANGE BARYON PRODUCTION IN  
SULPHUR-SULPHUR INTERACTIONS AT 200 GeV/c PER NUCLEON**

S. Abatzis<sup>1)</sup>, E. Andersen<sup>3)</sup>, A. Andrighetto<sup>10)</sup>, F. Antinori<sup>5)</sup>, A.C. Bayes<sup>4)</sup>,  
M. Benayoun<sup>6)</sup>, W. Beusch<sup>5)</sup>, J. Böhm<sup>7)</sup>, J.N. Carney<sup>4)</sup>, N. Carrer<sup>10)</sup>, B. de la Cruz<sup>9)</sup>,  
J.P. Davies<sup>4)</sup>, D. Di Bari<sup>2)</sup>, D. Elia<sup>2)</sup>, D. Evans<sup>4)</sup>, K. Fanebust<sup>3)</sup>, R. Fini<sup>2)</sup>,  
B.R. French<sup>5)</sup>, B. Ghidini<sup>2)</sup>, H. Helstrup<sup>5)</sup>, A.K. Holme<sup>3)</sup>, A. Jacholkowski<sup>5)</sup>,  
J. Kahane<sup>6)</sup>, V.A. Katchanov<sup>11)</sup>, J.B. Kinson<sup>4)</sup>, A. Kirk<sup>5)</sup>, K. Knudson<sup>5)</sup>, I. Králik<sup>7)</sup>,  
P. Ladrón de Guevara<sup>9)</sup>, J.C. Lassalle<sup>5)</sup>, V. Lenti<sup>2)</sup>, Ph. Leruste<sup>6)</sup>, R. Lietava<sup>4)</sup>,  
R.A. Loconsole<sup>2)</sup>, G. Løvholden<sup>3)</sup>, V. Manzari<sup>2)</sup>, M. Morando<sup>10)</sup>, F. Navach<sup>2)</sup>,  
J.L. Narjoux<sup>6)</sup>, K.L. Norman<sup>4)</sup>, F. Pellegrini<sup>10)</sup>, E. Quercigh<sup>5)</sup>, R. Ricci<sup>8)</sup>, L. Šándor<sup>7)</sup>,  
K. Šafařík<sup>5)</sup>, G. Segato<sup>10)</sup>, A.V. Singovsky<sup>11)</sup>, M. Sené<sup>6)</sup>, R. Sené<sup>6)</sup>, T.F. Thorsteinsen<sup>3)</sup>,  
J. Urbán<sup>7)</sup>, G. Vassiliadis<sup>1)</sup>, M. Venables<sup>4)</sup>, O. Villalobos Baillie<sup>4)</sup>, A. Volte<sup>6)</sup>,  
M.F. Votruba<sup>4)</sup>, and P. Závada<sup>7)</sup>.

**Abstract**

Strange and multistrange baryon and antibaryon production has been studied in sulphur sulphur interactions at 200 GeV/c per nucleon at central rapidity using the CERN Omega Spectrometer. Particle production ratios and transverse mass spectra are presented for  $\Lambda$ ,  $\Xi^-$ ,  $\bar{\Lambda}$  and  $\bar{\Xi}^-$ .

*(Submitted to Physics Letters B)*

---

<sup>1)</sup> Athens University, Athens, Greece.

<sup>2)</sup> Dipartimento di Fisica dell'Università and Sezione INFN, Bari, Italy.

<sup>3)</sup> Universitetet i Bergen, Bergen, Norway.

<sup>4)</sup> University of Birmingham, Birmingham, UK.

<sup>5)</sup> CERN, Geneva, Switzerland.

<sup>6)</sup> Collège de France and IN2P3, Paris, France.

<sup>7)</sup> Institute of Experimental Physics, Košice, Slovakia.

<sup>8)</sup> Laboratorio Nazionale di Legnaro, Legnaro, Italy.

<sup>9)</sup> CIEMAT, Madrid, Spain.

<sup>10)</sup> Dipartimento di Fisica dell'Università and Sezione INFN, Padua, Italy.

<sup>11)</sup> IHEP, Protvino, Russia.

The production of strange baryons and antibaryons is considered to be a useful probe of the dynamics of hadronic matter under extreme conditions of temperature and density[1, 2, 3]. The relative abundances for different species of baryons and antibaryons yield information about the nature of flavour equilibrium in the system formed in a heavy ion collision[2, 4, 5]. In addition, the transverse mass spectra can be used to provide independent estimates of temperature and to investigate collective flow. At equilibrium the strangeness yields are expected to be considerably higher than in pp interactions, whether or not a Quark-Gluon Plasma (QGP) is formed; however, the times required to achieve equilibrium are very different depending on whether the system undergoes a phase transition or not[2, 6]. A rapid increase in the number of strange quarks occurs if a QGP is formed, while the strangeness build-up in a purely hadronic system is much slower, owing to the small cross sections for strangeness-producing reactions. Strange and multistrange antibaryon production have particularly long equilibration times in a baryon-rich system which does not undergo a phase transition, as antibaryon production is in general disfavoured. In the absence of a phase transition, the hadronic system formed in a sulphur-sulphur interaction is not thought to live long enough to allow strange and multistrange antibaryons to reach their full equilibrium abundances. For this reason, it has been argued[7] that abundance ratios between strange antibaryons, such as  $\bar{\Xi}^-/\bar{\Lambda}$ , could be sensitive to a phase transition in the system in which the particles are produced.

Recently, string models have provided an alternative approach to strangeness production in heavy ion collisions. The basis of such models is the description of low  $p_T$  hadron-hadron collisions in terms of interactions between strings[8]. Additional production mechanisms (final state interactions, and, in the case of dense systems, a coalescence mechanism, such as colour rope formation[9], string fusion[10] or quark droplet formation[11]) have to be considered in order to account for the observed strangeness enhancement.

The WA94 experiment[12] is a dedicated experiment aimed at the study of strange particle spectra in sulphur-sulphur interactions. The experiment was performed at the CERN Omega Spectrometer. The data discussed in this paper were obtained using the Omega Multi-Wire Proportional Chambers (MWPC) in butterfly mode[13]. The layout of the apparatus is shown in figure 1. An incident sulphur beam, identified using a quartz Cerenkov counter, impinges on a 2% interaction length sulphur target. A downstream quartz Cerenkov counter ensures there is no outgoing sulphur ion. A pulse-height measurement in two scintillator counters placed above and below the beam, both covering the pseudorapidity interval  $2.2 \leq \eta \leq 3.5$ , is used to trigger on central interactions. Two 512 channel microstrip detectors, each with sensitive area  $2.5 \times 2.5 \text{ cm}^2$ , are placed behind the trigger scintillators in order to sample the charged particle multiplicity in this pseudorapidity interval. The Omega MWPCs and the target are positioned so as to select tracks coming from the target with a transverse momentum  $p_T \geq 0.6 \text{ GeV}/c$  in the rapidity interval  $2.4 \leq y_{\text{LAB}} \leq 3.2$ . A downstream hadron calorimeter is used to monitor forward energy. The trigger selects about 25% of the total inelastic cross section. The rapidity interval is chosen so as to give the same centre of mass rapidity coverage in sulphur-sulphur interactions as was used previously by the WA85 collaboration in sulphur tungsten interactions[14]. The apparatus is symmetric with respect to charge, giving equal acceptances for particles and antiparticles. However, data were taken with both

orientations of the magnetic field in order to check for residual systematic effects.

The selection procedure for  $V^0$ s and cascades is very similar to that previously used by the WA85 collaboration in SW interactions[14, 15], taking into account the modifications to the layout appropriate for sulphur sulphur interactions. Tracks reconstructed in the MWPCs are combined to search for  $V^0$  and cascade candidates. A pair of oppositely charged particles is considered as a  $V^0$  candidate if

1. the distance of closest approach between the two oppositely charged tracks is  $< 1.0$  cm,
2. each track traces through the seven MWPCs,
3. the angle between the  $V^0$  line of flight from the target and the sum of the three-momenta for the  $V^0$  decay tracks is  $< 0.75^\circ$ , *i.e.* the candidate comes from the target,
4. the decay distance is  $> 135$  cm,
5.  $|\alpha| > 0.45$ , where  $\alpha$  is the Podolanski-Armenteros[16] asymmetry parameter  $\alpha = (p_{L+} - p_{L-})/(p_{L+} + p_{L-})$ , and  $p_{L\pm}$  denotes the decay track momentum component parallel to the  $V^0$  momentum, and
6. the decay tracks, when traced back to the target plane, miss the target in the bend plane of the magnet; the impact parameters ( $\Delta y$ ) are required to be  $|\Delta y| > 2.0$  cm for the (anti)proton track, and  $|\Delta y| > 4.0$  cm for the pion.

These cuts yield the mass spectra shown in figures 2a and 2b.  $\Lambda$  ( $\bar{\Lambda}$ ) candidates are selected in a 50 MeV interval centred on the  $\Lambda$  mass, giving 56 140  $\Lambda$  and 18 014  $\bar{\Lambda}$  candidates.

Cascade candidates are selected by combining a  $\Lambda$  ( $\bar{\Lambda}$ ) with a decay pion in order to identify the decay sequence

$$\Xi(\bar{\Xi}) \rightarrow \Lambda(\bar{\Lambda})\pi; \Lambda(\bar{\Lambda}) \rightarrow p(\bar{p})\pi$$

We consider any combination of a  $\Lambda$  or  $\bar{\Lambda}$  with a charged track of appropriate sign as a cascade candidate if

1. the distance of closest approach between the line of flight of the  $\Lambda$  ( $\bar{\Lambda}$ ) and the charged track is  $< 1.6$  cm,
2. each decay track traces through the first four MWPCs (less restrictive than before),
3. the cascade decay distance is  $> 90$  cm,
4. the cascade candidate comes from the target ( $|\Delta y|$  of the cascade impact with respect to the target centre  $< 2.0$  cm),
5. the decay pion does not come from the target ( $|\Delta y| > 6.0$  cm for the decay track impact at the target plane), and
6. the  $\Lambda$  vertex is downstream of the  $\Xi^-$  vertex.

The  $V^0$  is not required to point back to the target when selecting cascade candidates. The resulting effective mass distributions for cascade candidates are shown in figures 2c and 2d. Clear peaks are seen at the  $\Xi^-$  and  $\bar{\Xi}^-$  positions with little background. 547  $\Xi^-$  and 278  $\bar{\Xi}^-$  candidates are obtained by selecting events in a 100 MeV interval centred on the  $\Xi^-$  mass.

The transverse mass distributions for  $\Lambda$ ,  $\bar{\Lambda}$ ,  $\Xi^-$  and  $\bar{\Xi}^-$  particles are shown in figure 3. In these distributions and for the rest of the analysis we have required  $0.45 < |\alpha| < 0.60$  for  $\Lambda$  and  $\bar{\Lambda}$  candidates, in order to avoid contamination from  $K^0$  decays. The distributions are obtained in the rapidity interval  $2.5 \leq y_{\text{LAB}} \leq 3.0$ , and are corrected for acceptance, unseen decay modes and reconstruction efficiencies. In addition, the  $\Lambda$  and  $\bar{\Lambda}$  distributions have been corrected for feed-down from  $\Xi$  and  $\bar{\Xi}$  decays. The distributions have been fitted using the expression[17]

$$\frac{1}{m_T^{3/2}} \frac{dN}{dm_T} = A \exp(-m_T/\tau).$$

The inverse slopes obtained are given in table 1. They are slightly lower than those obtained in a similar centre-of-mass rapidity interval ( $2.3 \leq y_{\text{LAB}} \leq 2.8$ ) by the WA85 collaboration[18].

The relative hyperon yields have also been determined. Ratios are presented in table 2 for  $2.5 \leq y_{\text{LAB}} \leq 3.0$  in three different intervals:  $1.2 \leq p_T \leq 3.0$  GeV/ $c$ ,  $1.0 \leq p_T \leq 2.0$  GeV/ $c$  and  $m_T \geq 1.9$  GeV. Columns 1 and 3 correspond to our best acceptance region and extrapolated values are given in column 2 in order to allow direct comparison with the pp data. It is interesting to note that using the trigger selections of WA94 the strangeness yield ratios obtained in sulphur-sulphur interactions are very similar to those obtained in sulphur-tungsten interactions by the WA85 collaboration in an equivalent centre-of-mass rapidity interval[18].

Figure 4 shows the ratios  $\Xi^-/\Lambda$  and  $\bar{\Xi}^-/\bar{\Lambda}$  for SS interactions (WA94) and SW interactions (WA85), together with those from other processes. Note that the ratio  $\bar{\Xi}^-/\bar{\Lambda}$  is three and a half times larger in both sulphur-induced reactions than the value ( $0.06 \pm 0.02$ ) obtained by the AFS collaboration in pp interactions[19], a 5 s.d. effect in each case.

In conclusion, results are presented for hyperon production in sulphur-sulphur interactions. The inverse slopes for  $\Lambda$ ,  $\bar{\Lambda}$ ,  $\Xi^-$  and  $\bar{\Xi}^-$  have values around 210 MeV, slightly lower than those obtained by the WA85 collaboration in SW interactions. Production ratios have been obtained for  $\Lambda$ s,  $\Xi$ s and their antiparticles. Similar ratios in SW interactions have been interpreted in terms of a sudden hadronization QGP model[20], and, more recently, in terms of string models with colour rope formation[21] or the Dual Parton Model with diquark-antidiquark pairs in the nucleon sea[22]. In addition a direct comparison with pp interactions shows that the ratio  $\bar{\Xi}^-/\bar{\Lambda}$  is considerably higher in sulphur-nucleus than in pp interactions.

## References

- [1] J. Rafelski and B. Müller, Phys. Rev. Lett. **48** (1982) 1066; **56** (1986) 2324.
- [2] P. Koch, B. Müller and J. Rafelski, Physics Reports **142** (1986) 167.
- [3] J. Ellis and U. Heinz, Phys. Lett. **262B**(1991)233.
- [4] T. Matsui, B. Svetitsky and L.D. McLerran, Phys. Rev. **D34** (1986) 2047.
- [5] K.S. Lee, M. Rhoades-Browne and U. Heinz, Phys. Rev. **C31**(1988) 1452.
- [6] E. Schnedermann and U. Heinz, Phys. Rev. Lett. **69** (1992) 2908.
- [7] J. Rafelski, Phys. Lett. **262B** (1991) 333.
- [8] K. Werner, in *Proc. ICPA-QGP'93*, ed. B. Sinha, Y.P. Viyogi and S. Raha. (World Scientific, Singapore, 1994.)
- [9] H. Sorge et al., in *Particle Production in Highly Excited Matter*, ed. H.H. Gutbrod and J. Rafelski, Plenum Press, New York, 1993.
- [10] N.S. Amelin et al., Phys. Rev. **C47** (1993) 2299.
- [11] K. Werner, Nucl. Phys. **A566** (1994) 477c.
- [12] WA94 proposal. CERN/SPSLC/91-5 P 257 (1991).
- [13] W. Beusch et al., Nucl. Inst. and Meth. **A249** (1986) 391.
- [14] S. Abatzis et al., Phys. Lett. **B244** (1990) 130.
- [15] S. Abatzis et al., Phys. Lett. **B270** (1991) 123.
- [16] J. Podolanski and R. Armenteros, Phil. Mag. **45** (1954) 13.
- [17] H.C. Eggers and J. Rafelski, Int. J. Mod. Phys. **A6** (1991)1067.
- [18] S. Abatzis et al., Nucl. Phys. **A566** (1994) 225c.
- [19] T. Åkesson et al., Nucl. Phys. **B246** (1984) 1.
- [20] J. Letessier et al., Phys. Rev. Lett. **70** (1993) 3530.
- [21] H. Sorge, SUNY-NTG-94-50, October 1994.
- [22] A. Capella, LPTHE Orsay 94-113, December 1994.

# Tables

Table 1: Inverse slopes of hyperons in SS interactions.

Particle	inverse slope (MeV)
$\Lambda$	$213 \pm 2$
$\bar{\Lambda}$	$204 \pm 5$
$\Xi^-$	$222 \pm 10$
$\bar{\Xi}^-$	$208 \pm 25$

Table 2: Relative hyperon yields in SS interactions  $2.5 < y < 3.0$

Ratio	$1.2 < p_T < 3.0 \text{ GeV}/c$	$1.0 < p_T < 2.0 \text{ GeV}/c$	$m_T > 1.9 \text{ GeV}/c$
$\bar{\Lambda}/\Lambda$	$0.23 \pm 0.01$	$0.24 \pm 0.01$	$0.22 \pm 0.01$
$\bar{\Xi}^-/\Xi^-$	$0.55 \pm 0.07$	$0.58 \pm 0.07$	$0.54 \pm 0.06$
$\Xi^-/\Lambda$	$0.09 \pm 0.01$	$0.08 \pm 0.01$	$0.18 \pm 0.01$
$\bar{\Xi}^-/\bar{\Lambda}$	$0.21 \pm 0.02$	$0.20 \pm 0.02$	$0.44 \pm 0.04$

## Figures

1. Layout of the WA94 experiment.
2. (a)  $p\pi^-$  effective mass distribution, (b)  $\bar{p}\pi^+$  effective mass distribution. (c)  $\Lambda\pi^-$  effective mass distribution, (d)  $\bar{\Lambda}\pi^+$  effective mass distribution.
3. Transverse mass distributions for (a)  $\Xi^-$  and  $\Lambda$ , and (b)  $\bar{\Xi}^-$  and  $\bar{\Lambda}$ .
4.  $\Xi^-/\Lambda$  and  $\bar{\Xi}^-/\bar{\Lambda}$  ratios for different reactions.

Figure 1:



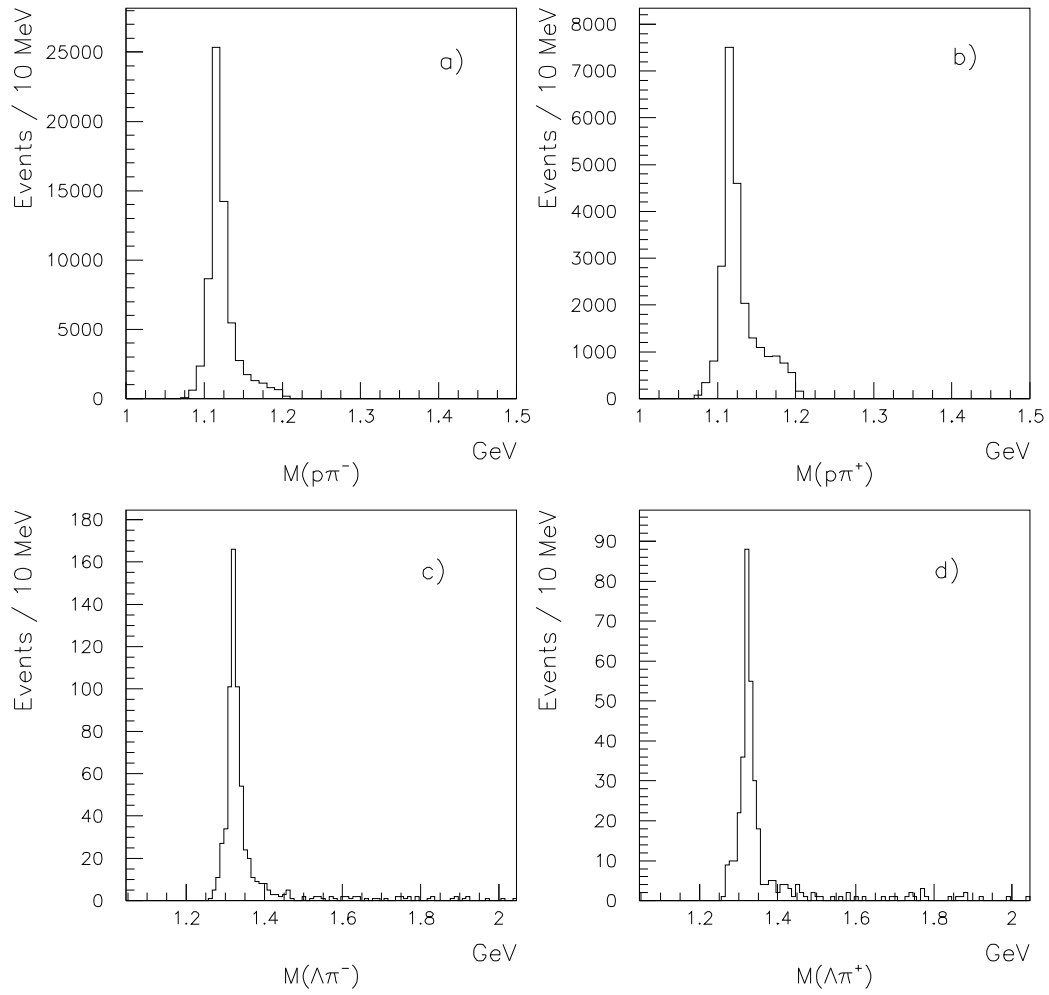


Figure 2:

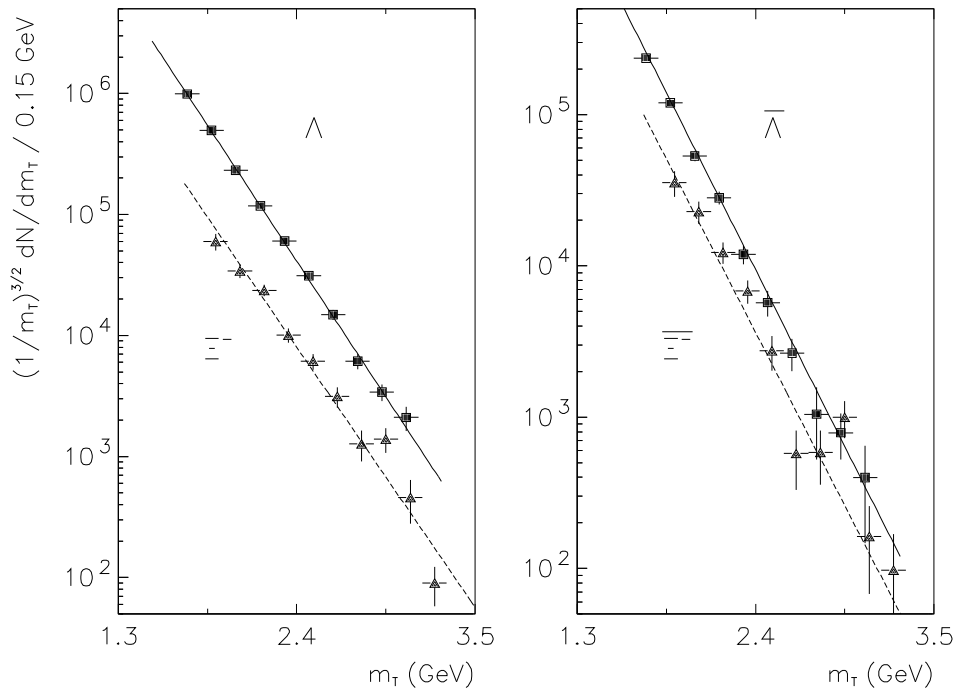


Figure 3:

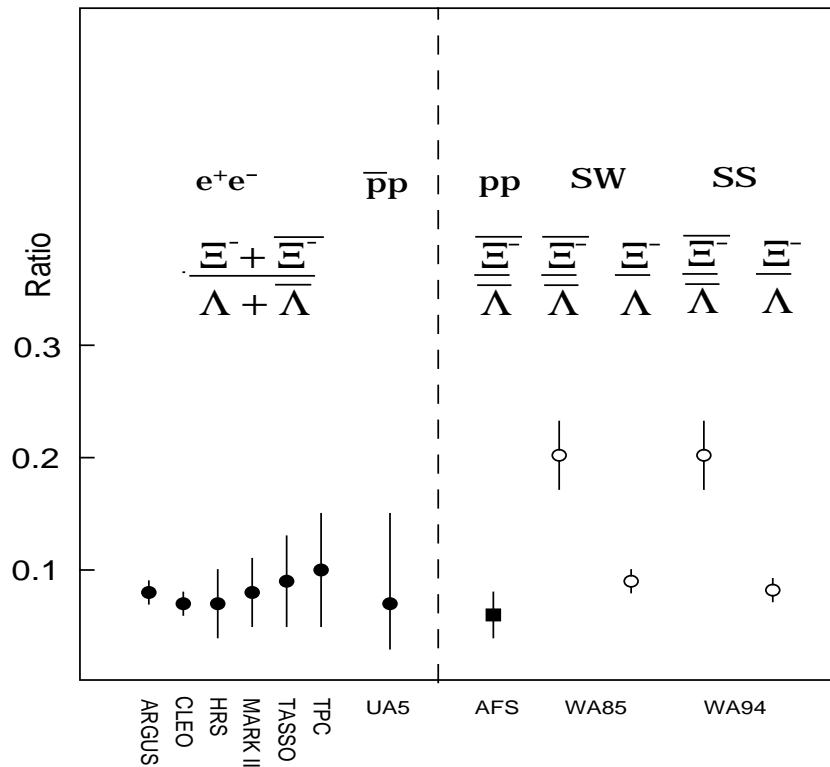


Figure 4: